JOURNAL OF MATERIALS SCIENCE **34** (1999) 4321–4328

Effects of pressure sensitivity on the η factor and the *J* integral estimation for compact tension specimens

A. AL-ABDULJABBAR, J. PAN
Mechanical Engineering and Applied Mechanics, The University of Michigan, Ann Arbor, MI 48109, USA
E-mail: jwo@engin.umich.edu

In this paper, the effects of pressure-sensitive yielding on the η factor and the *J* integral estimation for compact tension specimens are investigated. The analytical expressions for η and *J* for pressure-insensitive von Mises materials are generalized to pressure-sensitive Drucker-Prager materials using a lower bound approach. The η factor as a function of the pressure sensitivity and the normalized crack depth for compact tension specimens is derived under plane stress and plane strain conditions. The numerical results indicate that the η factor decreases as the pressure sensitivity increases. The effects are more pronounced under plane strain conditions than under plane stress conditions. However, the effects of the pressure sensitivity on η are found to be mild in general. For rigid perfectly-plastic materials, the *J* estimation for pressure-sensitive materials is also reduced to a simple expression of the tensile yield stress times the crack tip opening displacement as for the von Mises materials.

1. Introduction

The *J* integral, introduced by Rice [1, 2], has been widely used for the prediction of crack initiation where the linear elastic fracture mechanics (LEFM) theory cannot be used. The *J* integral was originally derived for deformation plasticity (nonlinear elastic) materials. From the viewpoint of energy release rate, *J* can be inferred from the experimental load-displacement curves of test specimens. Hence, it is possible to estimate the *J* integral from the load-displacement curves of various test specimen geometries (Begley and Landes [3, 4]). Bucci *et al.* [5] and Rice *et al.* [6] proposed the *J* estimation method for several specimen geometries, including compact tension specimens. Merkle and Corten [7] presented the *J* integral estimation for compact tension specimens using a limit load analysis by considering the effects of the combined loading of the axial force and the bending moment applied to the remaining ligament of the specimens. They used a lower-bound approach to derive the η factor for the *J* integral estimation. The η factor approach has been widely used to estimate the *J* integral from the area under the load-displacement (P-Δ) curve of a test specimen or structure

$$J = \frac{\eta}{b} \int P \, d\Delta, \tag{1}$$

where b is the remaining ligament of the specimen [8, 9].

For plastics, ceramics, some metal alloys such as nodular and malleable cast iron and even some steels, yielding is sensitive to pressure. The pressure-sensitive yielding is demonstrated by different values of the yield stress in tension and compression when the Bauschinger effect is not considered. This is contrary to the prediction of the von Mises yield criterion where the initial yield stress has the same magnitude under tension and compression. Recently, Dong *et al.* [16] investigated the fracture toughness of nodular cast iron using compact tension specimens. For nodular cast iron, the values of the yield stress in tension and compression are quite different. This indicates that pressure-sensitive yielding in nodular cast iron is not negligible. However, the lower-bound approach used in the work of Merkle and Corten [7] to estimate η and *J* is based on fully plastic yielding with the same value of the yield stress in tension and compression. Therefore, we here investigate the effects of pressure-sensitive yielding (demonstrated by different values of the yield stress in tension and compression) on η and the estimation of *J* for compact tension specimens of ductile pressure-sensitive materials under fully plastic yielding conditions.

In this work, we first investigate the effect of the pressure sensitivity on the lower-bound limit load for compact tension specimens. Then, analytical expressions for the η factor and the *J* integral for rigid perfectly-plastic materials are derived for compact tension specimens of pressure-sensitive materials. We also present a parallel analysis by considering the effects of plane strain conditions on the yield stresses under compression and tension for thick specimens. Finally, the effects of pressure sensitivity on η and *J* for rigid

perfectly-plastic materials are presented for different values of the normalized crack length and the pressure sensitivity.

2. Plastic limit load and *J* estimation

2.1. Drucker-Prager yield criterion

For pressure-sensitive materials, the hydrostatic pressure (or mean stress) affects yielding. To model pressure-sensitive yielding, Drucker and Prager [10] proposed a phenomenological yield criterion that is a linear combination of the effective stress and the mean stress. The Drucker-Prager yield criterion is a generalization of the Coulomb rule in soil mechanics where the shear stress required for simple slip is linearly dependent upon the normal pressure on the slip surface. The Drucker-Prager yield criterion [10, 11] is represented by

$$\sigma_e + \sqrt{3}\,\mu\sigma_m = \sigma_0, \tag{2}$$

where μ is the pressure sensitivity factor, σ_e is the effective tensile stress and σ_m is the mean stress. Here, σ_m is defined as $\sigma_m = \sigma_{kk}/3$ and σ_e is defined as $\sigma_e = (3s_{ij}\,s_{ij}/2)^{1/2}$ where s_{ij} are the deviatoric stress components. The deviatoric stresses are defined as $s_{ij} = \sigma_{ij} - \sigma_{kk}\delta_{ij}/3$. The subscripts i, j and k range from 1 to 3 and δ_{ij} is the Kronecker delta. Summation convention is adopted for repeated indices. In Equation 2, σ_0 is the generalized effective tensile stress. For perfectly plastic materials, σ_0 is a constant.

The value of the pressure sensitivity μ varies for different classes of materials. Spitzig *et al.* [12–14] reported that μ ranges from 0.029 to 0.064 for maraging and tempered martensitic steels. For malleable cast iron, μ is 0.22 [15]. For nodular cast iron, μ can have a value of 0.28 as reported in Dong *et al.* [16]. For polymers, Kinloch and Young [17] reported that μ ranges from 0.10 to 0.25. For zirconia-containing phase-transformation ceramics, much larger values of μ for phase transformation were reported. For example, μ ranges from 0.55 for Mg-PSZ [18] to 0.93 for Ce-TZP [19].

The generalized effective tensile stress σ_0 and the pressure sensitivity μ are related to the uniaxial tensile yield stress σ_t and the compressive yield stress σ_c by the following relations

$$\mu = \sqrt{3}\left(\frac{\sigma_c - \sigma_t}{\sigma_c + \sigma_t}\right), \tag{3}$$

and

$$\sigma_0 = \frac{2\sigma_c\sigma_t}{\sigma_c + \sigma_t}. \tag{4}$$

Define $\mu' = \mu/\sqrt{3}$. Then σ_t and σ_c can be expressed in terms of μ' and σ_0 as

$$\sigma_t = \frac{1}{1+\mu'}\sigma_0, \tag{5}$$

and

$$\sigma_c = \frac{1}{1-\mu'}\sigma_0. \tag{6}$$

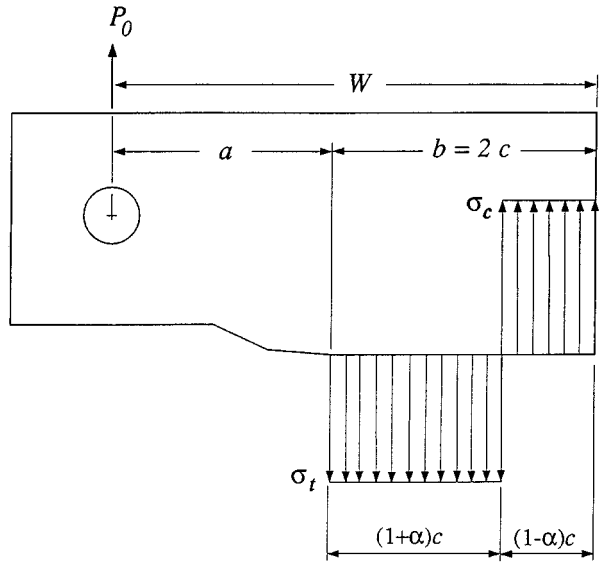

Figure 1 The geometry of a compact tension specimen and the stress diagram for the remaining ligament.

Equations 5 and 6 can also be obtained from the yield criterion of Equation 2 by considering uniaxial tensile and compressive loading, respectively.

2.2. Plastic limit load

Here, we use a lower-bound approach to obtain a limit load for compact tension specimen of pressure-sensitive materials as in Merkle and Corten [7]. Consider a compact tension specimen of perfectly plastic material as shown in Fig. 1. The specimen has a total width W, a crack length a, a remaining ligament size b and unit thickness. The specimen is loaded up to a fully plastic limit load P_0. The stress distribution in the remaining ligament of the specimen is assumed as shown in the figure where the portion of the ligament near the tip is under uniaxial tensile yield stress σ_t and the other portion is under uniaxial compressive yield stress σ_c. Here, we use a dimensionless parameter α which will be shown as a function of the crack depth and the pressure sensitivity.

The plastic limit load P_0 is obtained for the specimen with consideration of the force equilibrium in the vertical direction and the moment balance due to the in-plane force and stresses. The force equilibrium in the vertical direction requires

$$P_0 = c[(1+\alpha)\sigma_t - (1-\alpha)\sigma_c] \tag{7}$$

The moment due to the tensile and compressive stresses on the ligament as well as the limit load P_0 with respect to the point of stress reversal is

$$\frac{c^2}{2}\left[\sigma_t(1+\alpha)^2 + \sigma_c(1-\alpha)^2\right] - P_0[a + (1+\alpha)c] = 0. \tag{8}$$

In Equations 7 and 8, c is one half of the remaining ligament size b. A plastic limit load analysis for a specimen of pressure-sensitive materials under pure bending

is presented in the Appendix. Substituting Equation 7 into Equation 8 gives

$$2[\sigma_t(1+\alpha)-\sigma_c(1-\alpha)]-\left[\frac{a}{c}+(1+\alpha)\right] = \sigma_t(1+\alpha)^2+\sigma_c(1-\alpha)^2. \quad (9)$$

For pressure-insensitive Mises materials, the compressive and tensile yield stresses are the same. Therefore, $\sigma_t=\sigma_c=\sigma_0$, where σ_0 is the yield stress. Equation 9 can then be written as

$$\alpha^2+2\left(\frac{a}{c}+1\right)\alpha-1=0. \quad (10)$$

Solving Equation 10 for α gives

$$\alpha=\left[\left(\frac{a}{c}+1\right)^2+1\right]^{1/2}-\left(\frac{a}{c}+1\right). \quad (11)$$

Equations 10 and 11 are the same as those obtained by Merkle and Corten [7]. Note that for pressure-insensitive Mises materials, α is only a function of the crack depth.

For pressure-sensitive Drucker-Prager materials, the expressions for σ_t and σ_c from Equations 5 and 6 are used. Substituting these expressions into Equation 9, we get a governing equation for α for pressure-sensitive materials as

$$2\left[\frac{1}{1+\mu'}\sigma_0(1+\alpha)-\frac{1}{1-\mu'}\sigma_0(1-\alpha)\right] \times\left[\frac{a}{c}+(1+\alpha)\right]=\frac{1}{1+\mu'}\sigma_0(1+\alpha)^2 +\frac{1}{1-\mu'}\sigma_0(1-\alpha)^2. \quad (12)$$

Rearranging the above equation gives a quadratic equation for α as

$$\alpha^2+2\left(\frac{a}{c}+1\right)\alpha-\left[1+2\mu'\left(\frac{a}{c}+1\right)\right]=0. \quad (13)$$

Solving for α yields

$$\alpha=\left[\left(\frac{a}{c}+1\right)^2+1+2\mu'\left(\frac{a}{c}+1\right)\right]^{1/2}-\left(\frac{a}{c}+1\right). \quad (14)$$

When the pressure sensitivity factor μ is set to zero, the expression for α in Equation 14 reduces to Equation 11 for pressure-insensitive Mises materials, which was originally given by Merkle and Corten [7]. It is clear from Equation 14 that α is a function of the crack depth and the pressure sensitivity for pressure-sensitive materials.

For thick specimens, the plane strain conditions should be considered. In this case, the generalized effective stress is expressed in terms of the in-plane stresses as given by Li and Pan [20] as

$$\sigma_0=\frac{\sqrt{3}}{2}\left(1-\frac{\mu^2}{3}\right)^{1/2}\left[(\sigma_{11}-\sigma_{22})^2+4\sigma_{12}\right]^{1/2} +\frac{\sqrt{3}}{2}\mu(\sigma_{11}+\sigma_{22}), \quad (15)$$

where σ_{11} is the in-plane normal stress in the direction parallel to the crack, σ_{22} is the in-plane normal stress in the direction perpendicular to the crack, and σ_{12} is the in-plane shear stress. Denote σ_t^p as the tensile yield stress under plane strain conditions. Therefore, $\sigma_{22}=\sigma_t^p$ and $\sigma_{11}=\sigma_{12}=0$. Substituting these values into Equation 15 yields

$$\sigma_0=\frac{\sqrt{3}}{2}\left[\left(1-\frac{\mu^2}{3}\right)^{1/2}+\mu\right]\sigma_t^p, \quad (16)$$

from which σ_t^p can be expressed as

$$\sigma_t^p=\frac{\sigma_0}{\frac{\sqrt{3}}{2}\left[\left(1-\frac{\mu^2}{3}\right)^{1/2}+\mu\right]}. \quad (17)$$

Define two new parameters σ_0'' and μ'' as

$$\sigma_0''=\frac{\sigma_0}{\frac{\sqrt{3}}{2}\left(1-\frac{\mu^2}{3}\right)^{1/2}}, \quad (18)$$

$$\mu''=\frac{\mu}{\left(1-\frac{\mu^2}{3}\right)^{1/2}}. \quad (19)$$

Combining Equations 17–19 gives σ_t^p expressed in a form similar to that of σ_t in Equation 5 as

$$\sigma_t^p=\frac{1}{1+\mu''}\sigma_0'', \quad (20)$$

Similarly, the compressive yield stress σ_c^p under plane strain conditions can be obtained as

$$\sigma_c^p=\frac{1}{1-\mu''}\sigma_0''. \quad (21)$$

Equations 20 and 21 can be used to describe the tensile and compressive yield stresses under plane strain conditions. Note that the forms of the yield stresses in compression and tension under plane stress and plane strain conditions are similar, as demonstrated by Equations 5 and 6 on one hand and Equations 20 and 21 on the other hand. Therefore, analogous relations for the plane strain case can be obtained by using μ'' in stead of μ' for the plane stress case. Then we get a similar expression for α in terms of μ'' as

$$\alpha=\left[\left(\frac{a}{c}+1\right)^2+1+2\mu''\left(\frac{a}{c}+1\right)\right]^{1/2}-\left(\frac{a}{c}+1\right). \quad (22)$$

2.3. The η factor and J integral calculation

Rice *et al.* [6] gave the J integral expression in terms of the load-displacement (P-Δ) curve for deeply-cracked specimens as

$$J=\frac{2}{b}\int_0^{\Delta}P\,d\Delta. \quad (23)$$

The displacement Δ can be decomposed into an elastic part Δ_e and a plastic part Δ_p as

$$\Delta = \Delta_e + \Delta_p. \tag{24}$$

Then, J can be expressed as

$$J = J_e + J_p, \tag{25}$$

where J_e represents the elastic part of J, and J_p the plastic part of J. Merkle and Corten [7] expressed the plastic part J_p as

$$J_p = \frac{\eta}{b}\int_0^{\Delta p} P\, d\Delta_p + \frac{\eta^*}{b}\int_0^{p} \Delta_p\, dP, \tag{26}$$

where η and η^* are dependent on the geometry of the specimen and loading. The first and second integrals in Equation 26 are the plastic work and the complimentary plastic work done on the specimen, respectively.

The η factor is defined by

$$\eta = b\frac{1}{P_0}\frac{dP_0}{db}. \tag{27}$$

From Equations 5–7, P_0 is evaluated as

$$P_0 = \frac{2c\sigma_0}{1-\mu'^2}(\alpha - \mu'). \tag{28}$$

Differentiating P_0 with respect to b, with $dc/db = 1/2$, yields

$$\frac{dP_0}{db} = \frac{2c\sigma_0}{1-\mu'^2}\left(\alpha - \mu' + c\frac{\partial\alpha}{\partial c}\right). \tag{29}$$

Then, η can be obtained by substituting Equations 28 and 29 into Equation 27, with $b = 2c$, as

$$\eta = 1 + \frac{c}{\alpha - \mu'}\frac{\partial\alpha}{\partial c}. \tag{30}$$

In order to determine $\partial\alpha/\partial c$, Equation 13 is differentiated with respect to c using the relation $a = W - 2c$ to evaluate $\partial a/\partial c$

$$2\alpha\frac{\partial\alpha}{\partial c} + 2\left[\frac{-2c-a}{c^2}\alpha + \left(\frac{a}{c}+1\right)\frac{\partial\alpha}{\partial c}\right] - 2\mu'\frac{-2c-a}{c^2} = 0. \tag{31}$$

From Equation 31, the form needed in Equation 30 can be solved for as

$$\frac{c}{\alpha-\mu'}\frac{\partial\alpha}{\partial c} = \frac{2+\dfrac{a}{c}}{\alpha + \dfrac{a}{c} + 1}. \tag{32}$$

Equation 13 is again used to get the expression for a/c as

$$\frac{a}{c} = \frac{1 - 2(\alpha - \mu') - \alpha^2}{2(\alpha - \mu')}. \tag{33}$$

The expression for a/c in Equation 33 is then substituted into Equation 32 which yields

$$\frac{c}{\alpha-\mu'}\frac{\partial\alpha}{\partial c} = \frac{1 + 2(\alpha - \mu') - \alpha^2}{1 - 2\mu'\alpha + \alpha^2}. \tag{34}$$

Finally, substituting Equation 34 into Equation 30 and simplifying give the expression for η as

$$\eta = 2\frac{(1+\alpha)(1-\mu')}{1 - 2\mu'\alpha + \alpha^2}, \tag{35}$$

where α is expressed in Equation 14. We can compare the form for η in Equation 35 with the one given by Merkle and Corten for Mises materials (Equation 47 in Ref. [7]). It is clear that Equation 35 reduces to their expression when μ is set to zero. For the plane strain case, the expression for η takes a similar form to that of Equation 35 with μ'' replacing μ' as

$$\eta = 2\frac{(1+\alpha)(1-\mu'')}{1 - 2\mu''\alpha + \alpha^2}, \tag{36}$$

where α is expressed in Equation 22.

For rigid perfectly plastic materials, the elastic strain is zero, and so is the complimentary plastic work in Equation 26. Therefore, the J integral for the plane stress case reduces to

$$J = \frac{2}{b}\frac{(1+\alpha)(1-\mu')}{1 - 2\mu'\alpha + \alpha^2}P_0\Delta \tag{37}$$

Fig. 2 shows the displacement diagram for the compact tension specimen (see Merkle and Corten [7]). The applied displacement Δ can be related to the crack-tip opening displacement δ by

$$\frac{\Delta}{a + (1+\alpha)c} = \frac{\delta}{(1+\alpha)c}, \tag{38}$$

from which Δ is obtained as

$$\Delta = \frac{\left(\dfrac{a}{c}\right) + (1+\alpha)}{(1+\alpha)}\delta. \tag{39}$$

Combining Equations 28, 33, 37, and 39 gives an expression for the J integral for rigid perfectly-plastic pressure-sensitive mateials as

$$J = \frac{1}{1+\mu'}\sigma_0\delta = \sigma_t\delta, \tag{40}$$

where Equation 5 is used. For a material without pressure sensitivity, the resulting expression in Equation 40 is similar to the simple J integral expression for rigid perfectly-plastic Mises materials.

For the plane strain case, the expression for J is derived in terms of μ'' and σ_0'', instead of μ and σ_0. In this case. Equation 20 is used in the result in order to obtain J in terms of the tensile yield stress σ_t^p under plane strain conditions as

$$J = \sigma_t^p\delta. \tag{41}$$

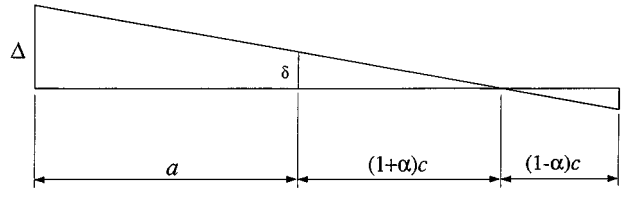

Figure 2 Relation between the applied displacement Δ and the crack-tip opening displacement δ for rigid-perfectly plastic material as in Merkle and Corten [7].

It is noted that the J integral for rigid perfectly-plastic pressure-sensitive materials given by Equations 40 and 41 is independent of the value of a/c, as for Mises materials. Equations 40 and 41 are in agreement with the results for the Dugdale-Barenblatt cohesive zone model for perfectly-plastic materials.

3. Numerical results and discussions

Although the relations developed earlier for the η factor are for the idealized case of rigid perfectly-plastic material behavior, they are indicative of the role of the pressure sensitivity on the estimation of the J integral using the η factor approach. The J integral estimation procedure and the use of the η factor for compact tension specimens were originally intended to apply to metals [9]. The recent study of Dong *et al.* [16] on the fracture mechanisms in compact tension specimens of nodular cast iron motivates us to investigate the quantitative effects of the pressure sensitivity on the η factor for estimation of the J integral for pressure-sensitive metals under fully yielded conditions.

The relations derived for the η factor for pressure-sensitive materials are used here to depict the dependence of η on μ and the normalized crack length a/W. First, it is desirable to relate the variables here to the ratio of the crack length to the total specimen width, a/W, instead of the ratio a/c. Since the parameter α in Equation 14 is expressed in terms of a/c, we refer to the specimen geometry as shown in Fig. 1 to relate a/c to a/W by

$$\frac{a}{c} = \frac{2\left(\frac{a}{W}\right)}{1-\left(\frac{a}{W}\right)}, \tag{42}$$

which is used in the computation of α and η.

Figs 3 and 4 show the dependence of the η factor on the pressure sensitivity μ for the plane stress and plane strain cases, respectively. Fig 3 shows the η factor as a function of μ for three different values of $a/W = 0.2$, 0.5, and 0.8 for the plane stress case in which μ' is used in the calculations. It is shown in the figure that as the pressure sensitivity increases, the value of η decreases. This effect is mild in general, but it is more significant for small values of a/W than for large values. When a/W becomes large, the effect of the pressure sensitivity becomes less significant because for deeply-cracked specimens, η approaches the value of 2 regardless of the material constitutive behavior (Rice *et al.* [6]). For example, for $\mu = 0.3$, η is reduced from that for $\mu = 0$ by about 4% for $a/W = 0.2$, while it is reduced by about 1% for $a/W = 0.8$.

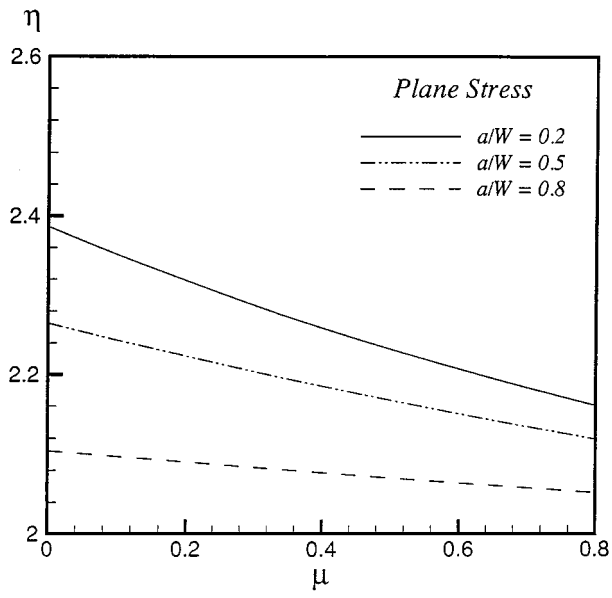

Figure 3 The η factor as a function of the pressure sensitivity μ for different values of a/W for the plane stress case.

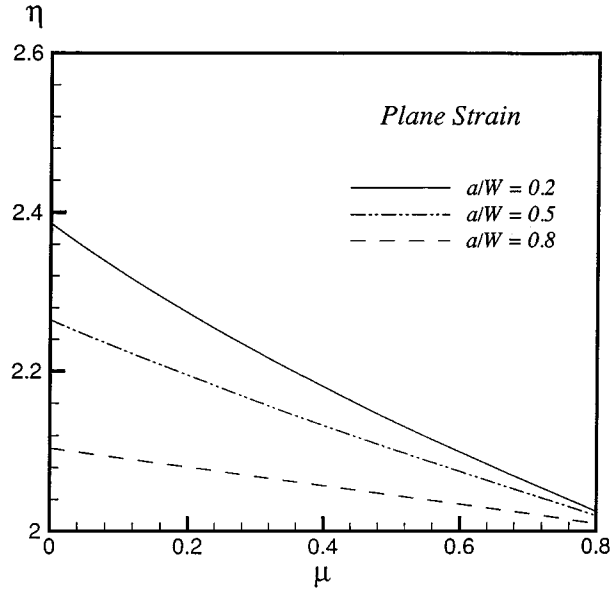

Figure 4 The η factor as a function of the pressure sensitivity μ for different values of a/W for the plane strain case.

Fig. 4 shows the η factor as a function of the pressure sensitivity μ for the same values of a/W as in Fig. 3 for the plane strain case, in which the calculations are made based on μ''. Comparing with Fig. 3 for the plane stress case, we find that while in both cases the values of η emanate from the same values at $\mu = 0$ for different values of a/W and decrease with increasing μ, the rate of decrease of η in the plane strain case is higher, and thus the effect of the pressure sensitivity is more prominent. For example, for $a/W = 0.2$, η for $\mu = 0.3$ is reduced from that for $\mu = 0$ by about 7% in Fig. 4 as opposed to the 4% as noted for the plane stress case. For $a/W = 0.5$, η for $\mu = 0.3$ is reduced from that for $\mu = 0$ by about 4.5%. The same trend of a mild effect of the pressure sensitivity on η for larger values of a/W for the plane stress case as shown in Fig. 3 is also seen here. However, the value of η for the plane strain case approaches 2 for all ratios a/W at a higher rate than that for the plane stress case as μ increases.

Figs 5 and 6 show the dependence of the η factor on the normalized crack length a/W for different values of μ. Fig. 5 is a plot of the η factor as a function of a/W for the plane stress case. For all the values of the pressure sensitivity, as a/W increases, the η factor decreases. For larger values of pressure sensitivity, ($\mu = 0.8$), the initial value of η is lower and closer to 2 and, consequently, η becomes relatively insensitive to

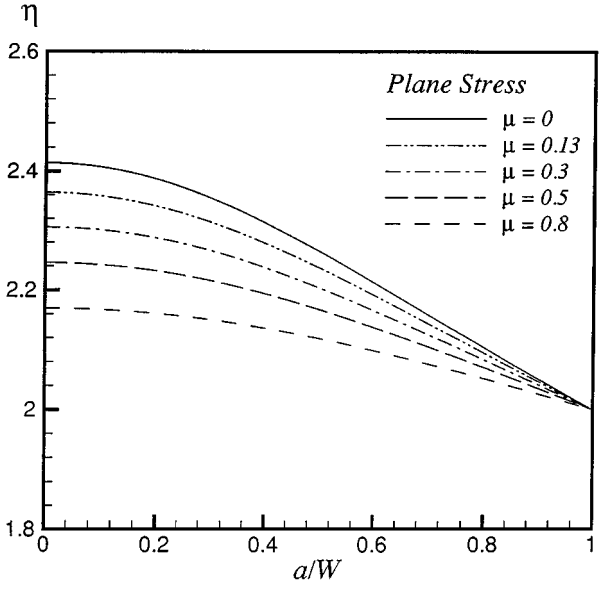

Figure 5 The η factor as a function of the normalized crack length a/W for different values of the pressure sensitivity μ for the plane stress case.

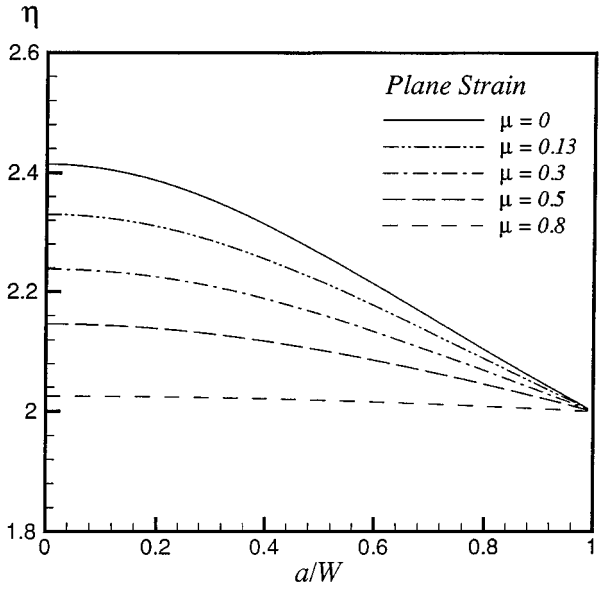

Figure 6 The η factor as a function of the normalized crack length a/W for different values of the pressure sensitivity μ for the plane strain case.

the value of a/W. This can also be observed in Fig. 3. Fig. 6 is a plot of the η factor as a function of a/W for the plane strain case. Comparing Fig. 6 with Fig. 5, we find that for $\mu = 0$, η remains the same for both of the cases. This is expected since when $\mu = 0$, η becomes a function of a/W only for both the plane stress and plane strain cases. Also, for a larger value of μ, the η factor is less sensitive to a/W in the plane strain case. As in the plane stress case, η for various pressure sensitivities approaches 2 for deep cracks.

The effect of the pressure sensitivity on the η factor is due to the fact that the introduction of the Drucker-Prager yield criterion induces a shift of the neutral axis of the remaining ligament of the specimen by accounting for the difference in the tensile and compressive yield stresses. A comparison between the von Mises yield criterion and the Drucker-Prager yield criterion for $\mu = 0.13$ is shown in Fig. 7 where both of the criteria are plotted in the two-dimensional principal stress $\sigma_1 - \sigma_2$ plane. The plots are normalized by the uniaxial tensile yield stress σ_t. In the figure, the Mises yield criterion is represented by the dashed line, and the Drucker-Prager criterion for a presure-sensitive material with $\mu = 0.13$ is represented by the solid line. Considering the plane stress case with $\sigma_2 = 0$, we see that in the Mises case, the normalized tensile and compressive yield stresses have the same magnitude. However, in the Drucker-Prager case, the uniaxial compressive yield stress is larger than the uniaxial tensile yield stress.

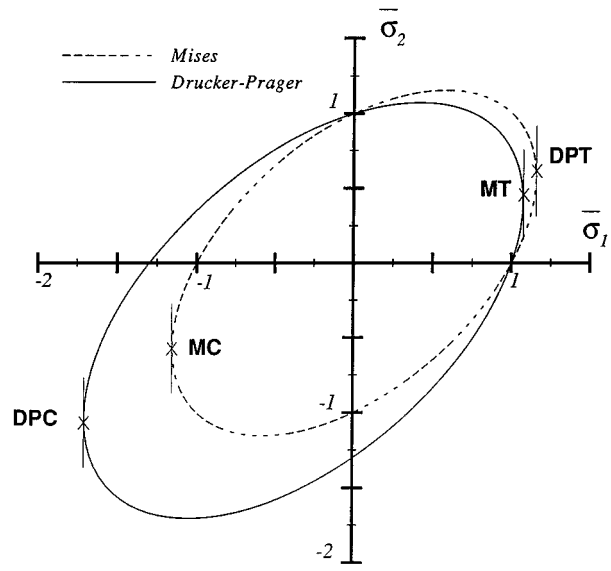

Figure 7 Yield contours based on the von Mises yield criterion and the Drucker-Prager yield criterion with $\mu = 0.13$ in the two dimensional principal stress plane.

Now we consider the plane strain case with $\epsilon_2 = 0$. Based on the normality flow, the tensile and compressive yield stresses are represented by points MT and MC on the yield contour for the Mises materials, where the outward normal to the yield contour is parallel to the σ_1 axis. On the other hand, the tensile and compressive yield stresses are represented by point DPT and DPC on the yield contour for the Drucker-Prager materials. The difference between the tensile and compressive yield stresses is much larger for the plane strain case than for the plane stress case. Therefore, the effects of the pressure sensitivity on η is larger for the plane strain case.

Note that the η factor in Equations 35 and 36 becomes undefined when $\mu' = 1.0$ and $\mu'' = 1.0$, respectively. Therefore, when evaluating η at $\mu' = 1.0$ from Equation 35 and $\mu' = 1.0$ from Equation 36, we resort to L'Hopital's rule. For both cases, the result is $\eta = 2$. These correspond to $\mu = \sqrt{3} = 1.73$ in the plane stress case, and $\mu = \sqrt{3}/2 = 0.866$ in the plane strain case. Mathematically speaking, this is why in the latter case, the effect of pressure sensitivity is more pronounced because it takes a lower value of the pressure sensitivity to reach to the limit value of η. This is due to the way the Drucker-Prager yield criterion is defined for the two cases. In the plane strain case, the difference between the comprssive and tensile yields, stresses is twice as much as it is in the plane stress case. The shift in the neutral axis in the remaining ligament increases in the plane strain case.

Even though the results presented here for the η factor are for the idealized case of rigid perfectly-plastic material behavior, they are indicative of the role of the pressure sensitivity on the estimation of the J integral. For materials with very small pressure sensitivity, the effect is mild. However, for materials where the pressure sensitivity is moderate, such as malleable and nodular cast irons, the effect is more noticeable and the difference in the calculation of the η factor for the estimation of the J integral for the compact specimen should be taken into consideration. For such types of materials, the η factor presented here is needed to estimate J.

4. Conclusions

In this work, we investigate the effect of pressure sensitivity on the η factor and the J integral estimation for compact tension specimens of rigid perfectly plastic materials. The η factor decreases with increasing pressure sensitivity for different crack lengths in general. However, the effect is mild for small and moderate values of pressure sensitivity. The effects of pressure sensitivity on η are found to be more pronounced for the plane strain case than for the plane stress case due to the larger difference between the tensile and compressive yield stresses in the plane strain case.

Acknowledgement

AA acknowledges the financial support of the Technical College of Riyadh, Riyadh, Saudi Arabia. JP acknowledges the initial support of this work by the NSF under grant number DMR-8708405.

Appendix: a limit moment analysis for bend specimens of pressure-sensitive materials

The limit moment for specimens of pressure-sensitive materials under pure bending can be obtained by considering the equilibrium under fully plastic load. Consider the specimen of unit thickness shown in Fig. 8 subjected to pure bending moment. A simple stress diagram for the left part of the specimen under fully plastic loading is also shown in the figure. Due to the pressure sensitivity, the compressive yield stress σ_c is larger than the tensile yield stress σ_t. Consequently, the span of the tensile portion with the width γb is larger than that of the compressive portion with the width $(1-\gamma)\ b$ in order to satisfy the force equilibrium. Therefore,

$$\gamma b\sigma_t - (1-\gamma)b\sigma_c = 0. \tag{43}$$

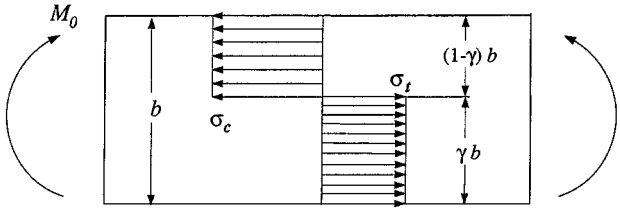

Figure 8 The geometry of a bend specimen subjected to pure bending and the stress diagram for the left part of the specimen for pressure-sensitive materials.

The moment balance with respect to the point of stress reversal is obtained as

$$M_0 = \gamma b\sigma_t\frac{\gamma b}{2} + (1-\gamma)b\sigma_c\frac{(1-\gamma)b}{2}. \tag{44}$$

For the plane stress case, σ_t and σ_c are given by Equations 5 and 6. Substituting the two equations into Equation 43 gives the expression for γ as

$$\gamma = \frac{(1+\mu')}{2} \tag{45}$$

Substituting this expression for γ into Equation 44 yields

$$M_0 = \frac{1}{4}\sigma_0 b^2. \tag{46}$$

This is the same as that for pressure-insensitive von Mises materials. However, σ_0 is the generalized tensile effective stress. For pressure-sensitive materials, σ_0 can be expressed as a function of the tensile yield stress σ_t and the pressure sensitivity μ from Equation 5. Then, M_0 becomes

$$M_0 = \frac{1}{4}(1+\mu')\sigma_t b^2. \tag{47}$$

Under plane strain conditions, the tensile yield stress σ_t^p and the compressive yield stress σ_c^p, given in Equations 20 and 21, should be used in Equations 43 and 44. In this case, the parameter γ becomes

$$\gamma = \frac{(1+\mu'')}{2} \tag{48}$$

The resulting moment becomes

$$M_0 = \frac{1}{2\sqrt{3}}\sigma_0'' b^2, \tag{49}$$

or, in terms of σ_0

$$M_0 = \frac{1}{\left(1-\frac{\mu^2}{3}\right)^{1/2}}\frac{1}{2\sqrt{3}}\sigma_0 b^2. \tag{50}$$

For $\mu = 0$, the first quotient in Equation 50 becomes unity, and the moment reduces to the expression for Mises materials. Similarly, M_0 can be expressed in terms of σ_t as

$$M_0 = \frac{1}{2\sqrt{3}}\frac{1+\mu'}{\left(1-\mu'^2\right)^{1/2}}\sigma_t b^2. \tag{51}$$

From Equations 47 and 51, the effects of pressure sensitivity on M_0 can be observed. As μ increases, M_0 increases because the compressive yield stress σ_c is larger than the tensile yield stress σ_t. Consequently, the loading needed to attain fully plastic conditions is larger.

References

1. J. R. RICE, *J. Appl. Mech.* **35** (1968) 379.
2. *Idem.*, in "Fracture II," edited by H. Liebowitz (Academic Press, 1969) p. 191.
3. J. A. BEGLEY and J. D. LANDES, in "Fracture Toughness," Proceedings of the 1971 National Symposium on Fracture Mechanics, Part II, ASTM STP 514 (American Society for Testing and Materials, 1972) p. 1.

4. J. D. LANDES and J. A. BEGLEY, in "Fracture Toughness," Proceedings of the 1971 National Symposium on Fracture Mechanics, Part II, ASTM STP 514 (American Society for Testing and Materials, 1972) p. 24.
5. R. J. BUCCI, P. C. PARIS, J. D. LANDES and J. R. RICE, in "Fracture Toughness," Proceedings of the 1971 National Symposium on Fracture Mechanics, Part II, ASTM STP 514 (American Society for Testing and Materials, 1972) p. 40.
6. J. R. RICE, P. C. PARIS and J. G. MERKLE, in "Progress in Flaw Growth and Fracture Toughness Testing," ASTM STP 536 (American Society for Testing and Materials, 1973) p. 231.
7. J. G. MERKLE and H. T. CORTEN, *J. Press. Vess. Tech., Trans. ASME* (1974) 286.
8. C. E. TURNER, in "Fracture Mechanics: Twelfth Conference," STP 700 (American Society for Testing and Materials, 1980) p. 314.
9. ASTM, "Standard Test Method for J_{IC}, a Measure of Fracture Toughness," E 813-89$^{\epsilon 1}$ (American Society for Testing and Materials, Philadelphia 1989) p. 713.
10. D. C. DRUCKER and W. PRAGER, *Q. Appl. Math.* **10** (1952) 157.
11. D. C. DRUCKER, *Metall. Trans.* **4** (1973) 667.
12. W. A. SPITZIG, R. J. SOBER and O. RICHMOND, *Acta Metall.* **23** (1975) 885.
13. *Idem., Metall. Trans.* **7A** (1976) 1703.
14. O. RICHMOND and W. A. SPITZIG, in "International Union of Theoretical and Applied Mechanics," 1980, p. 377.
15. J. A. COLLINS, in "Failure of Materials in Mechanical Design" (John Wiley & Sons, New York, 1981).
16. M. J. DONG, C. PIOUR and D. FRANCOIS, "Damage Influence on the Fracture Toughness of Nodular Cast Iron: Part II," *Metall. Mater. Trans.* (1997), in press.
17. A. J. KINLOCH and R. J. YOUNG, in "Fracture Behavior of Polymers" (Elsevier Applied Science, London, 1983).
18. I.-W. CHEN, *J. Amer. Ceram. Soc.* **74** (1991) 2564.
19. C.-S. YU and D. SHETTY, *ibid.* **72** (1989) 921.
20. F. Z. LI and J. PAN, *J. Appl. Mech.* **57** (1990) 40.

Received 30 April 1997
and accepted 24 February 1999